# A Novel Flower Pollination Based Global Maximum Power Point Method for Solar Maximum Power Point Tracking

J. Prasanth Ram and N. Rajasekar, *Member, IEEE*

***Abstract*—To maximize solar photovoltaic (PV) output under dynamic weather conditions, maximum power point tracking (MPPT) controllers are incorporated in solar PV systems. However, the occurrence of multiple peaks due to partial shading adds complexity to the tracking process. Even though conventional and soft computing techniques are widely used to solve MPPT problem, conventional methods exhibit limited performance due to fixed step size, whereas soft computing techniques are restricted by insufficient randomness after reaching the vicinity of maximum power. Hence, in this paper, a new flower pollination algorithm (FPA) with the ability to reach global peak is proposed. Optimization process in FPA method performs global and local search in single stage and it is a key tool for its success in MPPT application. The ruggedness of the algorithm is tested with zero, weak, and strong shade pattern. Further, comprehensive performance estimation via simulation and hardware are carried out for FPA method and are quantified with conventional perturb and observe and particle swarm optimization (PSO) methods. Results obtained with FPA method show superiority in energy saving and proved to be economical.**

***Index Terms*—Global maximum power point (GMPP), irradiation change (IC), local MPP (LMPP), photovoltaic (PV).**

## I. Introduction

CONTINUOUS increase in energy demand and depletion of fossil fuels has propelled world's attention toward inexhaustible power generation in the recent years [1], [2]. To encourage renewable power generation, the government has raised subsidies and introduced tariff-free schemes as initiation toward pollution-free power generation [3], [4]. Among the various forms of clean energy resources, solar energy is prioritized for its plenty availability and prominent features. Further, large solar power parks via solar photovoltaic (PV) have attracted the investor's attention around the globe.

Solar PV is a device that absorbs the incident photon energy and converts it into electrical power. Since the electrical characteristic of solar PV is nonlinear in nature, optimal performance is not assured when rapid weather conditions occur. To maximize PV output under dynamic weather conditions, solar PV systems incorporate MPPT controllers. These controllers use dc–dc converters for continuous power tracking.

Over the decades, research on maximum power point tracking (MPPT) remains active. Two common methodologies followed to reach maximum power point (MPP) are 1) conventional MPPT (CMPPT) [5]–[18] and 2) soft computing (SC) methods [19]–[26]. CMPPT method comprises of timeworn techniques that include: perturb and observe (P&O) [5]–[8], incremental conductance (INC) [12], [13], fractional short circuit [14], fractional open circuit [15], and ripple correlation control [16]. Despite their ability to yield good results under constant environmental conditions, they fail miserably under varying weather conditions due to their inherent drawbacks such as 1) poor convergence, 2) inability to reach global peak under partial shading condition, and 3) high-power frequency oscillations around MPP due to fixed step size [2]. To improve CMPPT method's performance: 1) adaptive, 2) two stage P&O, and 3) DIRECT search MPPT techniques have been put forward by researchers in [10], [17], and [18]. In two stage P&O method, the optimized zone for MPP operation is first detected and later on possibilities to make it operate at MPP is carried out [17]. While in case of DIRECT search method, two-way tracking strategies were adopted. Typically, during initial stage of the computation Global MPP mode (GMPP) is turned on and after reaching global peak the mode is switched back to the conventional P&O method [18]. Except adaptive method, both two step and DIRECT search method continue to have the drawback of fixed perturbation. Since these methods follow two stages of computation, the methods are rendered ineffective.

In the recent years, acknowledging the superiority in solving nonlinear optimization problems, SC techniques that adopt bio-inspired and evolutionary principles have been proposed for MPPT applications. Evolutionary algorithms such as fuzzy logic control (FLC) and artificial neural network (ANN) were first attempted in PV tracking in [19] and [20]. Besides its advantages, ANN method requires separate sensor arrangement to sense temperature changes, whereas complex design of fuzzy rules in FLC method requires prior system knowledge [2]. Taking these shortcomings into consideration, advanced metaheuristic methods such as genetic algorithm and artificial immune system were used for solving MPP problem [21], [22]. Despite their

Manuscript received June 10, 2016; revised August 16, 2016 and October 19, 2016; accepted December 16, 2016. Date of publication December 26, 2016; date of current version June 23, 2017. This work was supported under the development of the Solar Energy Research Cell by the administration of VIT University-Vellore. Recommended for publication by Associate Editor M. Vitelli.

The authors are with the Solar Energy Research Cell, School of Electrical Engineering, Vellore Institute of Technology, Vellore 632014, India (e-mail: jkprasanthram@gmail.com; natarajanrajasekar@gmail.com).

Color versions of one or more of the figures in this paper are available online at http://ieeexplore.ieee.org.

Digital Object Identifier 10.1109/TPEL.2016.2645449

robustness to solve nonlinear stochastic problem, time involved for computation is quite high, which reduces the convergence speed [2], [23].

Recently, the research groups working on MPPT methods had witnessed the excellence of swarm optimized and bio-inspired methods [23]–[33]. With the application of these methods, research on solar PV is kept one notch ahead and the problem of reaching the global peak is resolved convincingly. Generally, swarm optimization methods follow techniques that are derived from the natural behavior of flocks, fish pools, and birds [23], [24]. The major advantages associated with these methods are 1) starts with random search, 2) effectively avoid convergence toward local minima, and 3) easy implementation. The first successful swarm-based method implemented for MPPT application is the particle swarm optimization (PSO) method [23], [24]. Application of PSO method has convincingly solved the most important issue of steady state oscillations around MPP. However, this method loses its diversity once randomness is reduced [2]. Moreover, parameter initialization is also a tedious process involved in PSO technique [2], [26]–[28]. To handle this issue, a new deterministic PSO and modified PSO methods were proposed in [25] and [26], respectively. But the authors failed to showcase the performance of these methods under dynamic irradiated conditions. Besides, the procedure followed for particle initialization also makes it difficult to implement. In the recent times, bio-inspired methods are conceived well as an alternative to swarm methods. Cuckoo search [27], firefly algorithm [28], random search method (RSM) [29], artificial bee colony methods [30], ant colony optimization [31], and grey wolf optimization [32] are some of the important methods proposed in the field of MPPT. In addition to the above methods, a new deferential evolution PSO (DEPSO) fusing the properties of metaheuristic differential evolution and PSO method is also attempted for MPPT problem [33]. All these methods have shown quick convergence, accurate tracking, and fewer transients. Yet, drawbacks such as 1) procedural complexity, 2) increased effort for parameter tuning, and 3) insufficient randomness persist with these methods too.

To summarize 1) conventional method show limited performance due to fixed step size. 2) Adaptive and two-stage method suffers due to high complexity in implementation. 3) SC methods are restricted by insufficient randomness after reaching the vicinity of MPP along with high obscurity in parameter tuning. As an attempt to handle the aforementioned drawbacks, a new method named flower pollination algorithm (FPA) is proposed for MPPT applications. This method has several distinguished virtues such as 1) ability to explore as well as exploit the search space, 2) very less complexity, 3) easy to code and compile, and 4) lesser effort needed in parameter tuning. Further, two modes of search ability for accomplishing quick convergence are a key tool for its success. This value added advantages of FPA method is well exploited by the authors to make it utilize for constructing fast, reliable, and rugged MPPT method. In addition, the authors believe that this method can be tailored to suit the MPPT application. Underneath, to establish the performance of the FPA MPPT method, three different sets of test pattern covering various atmospheric conditions are evaluated via hardware and software simulation. The results obtained are further benchmarked with standard PSO and P&O methods. To portray FPA's superiority, a comparative study covering different parameters such as tracking speed, efficiency, parameter tuning, panel independency, and steps involved in tuning is made between various conventional and SC methods. Finally, a comprehensive quantitative comparison on revenue generation via energy saving with FPA method is also established. The remaining part of the paper is organized as follows.

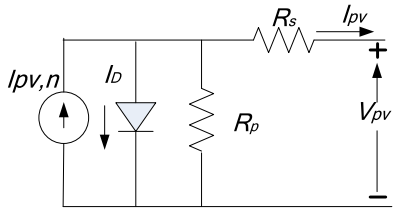


Fig. 1. Schematic of one-diode solar PV model.

Section II explains the modeling of solar PV, Section III describes the control structure of the proposed methodology with detailed steps on FPA–MPPT implementation. In Section IV, simulation studies with different shading patterns and step change in irradiation conditions are analyzed. Hardware realization via prototype model is presented in Section V. Comprehensive comparative study between proposed and various MPPT methods based on factors governing the implementation of MPPT is provided in Section VI. To highlight the importance of FPA, a quantitative performance analysis is carried out in terms of energy saved, economy, income generated, payback period, and net energy yield are presented in Section VII. Finally, conclusions derived are presented at the end.

## II. Modeling of Solar PV

In solar PV system modeling, cell model assumes importance since, the prediction of system performance mainly depends on accuracy of cell characteristics. To predict cell characteristics, two main modeling approaches that exist are 1) one-diode model and 2) two-diode model [5], [6]. In spite of the fact that two diode is more accurate, the author's in this paper have used one diode model just to avoid complexity [7], [8]. The schematic of one-diode model is shown in Fig. 1.

Applying KCL, The output current equation of solar PV cell is given by

$$I_{\mathrm{PV}} = I_{\mathrm{PV}n} - \left(I_O\left(e^{V_D/aV_T} - 1\right)\right) - \frac{V_{\mathrm{PV}} + I_{\mathrm{PV}}R_s}{R_p}. \quad (1)$$

In case of one-diode modeling, the five unknown model parameters are $I_{\mathrm{PV}n}, I_D, R_S, R_P, anda$, where, "$I_{\mathrm{PV}n}$" represents PV panel current, "$R_S, R_P$" indicate the series and parallel resistance, respectively, and $I_O\left(e^{V_D/aV_T} - 1\right)$ denotes the diode current "$I_D$," where "$V_D$" is the diode voltage, "$I_O$" is the reverse saturation current, "$a$" is the diode ideality factor, and "$V_T$" is the thermal voltage at any temperature and it is given by

$$V_T = \frac{N_S kT}{q}. \quad (2)$$

Here "$N_S$" is the number of cells connected in series, "$k$" the Boltzmann constant ($1.3805\times10^{-23}$ C), "$T$" temperature at STC (Standard Test Conditions) and "$q$" is the charge of electron ($1.9\times10^{-19}$ C). The module (or) panel current of the solar PV can be determined from the following equation:

$$I_{\rm PV} = N_{\rm pp}\left\{I_{{\rm PV},n} - I_O\left[\exp\left(\frac{V_{\rm PV}+I_{\rm PV}R_S}{V_t N_{\rm ss}}\right)-1\right]\right\} - \left(\frac{V_{\rm PV}+I_{\rm PV}R_S}{R_P}\right) \tag{3}$$

where "$I_{\rm PV}$" the module current, "$I_{{\rm PV},n}$" is the PV current, "$N_{\rm SS}$" and "$N_{\rm PP}$" are the number of cells connected in series and parallel to form a module, respectively.

## III. FPA and Its Implementation

### A. Partial Shaded Conditions (PSC) and Effects

Generally, a PV module is comprised of PV cells connected in series and parallel fashion. To meet the energy demand, in a similar way, PV array is constructed with series and parallel connected modules. The selection of interconnection schemes depends upon factors such as expected energy yield, performance, PV material, and complexity [35], [36]. Irrespective of the connection type, a common phenomenon occurring in a PV array that affects PV output is partial shading. The term partial shading refers to uneven distribution of irradiation across the panel and it occurs in a PV array due to any of the following reasons: 1) tree and building shadow, 2) movement of clouds, and 3) bird droppings [25], [26]. To demonstrate the phenomenon of shading and its consequence effects, a string of four panels (4S) in series with three different shade patterns, i.e., zero, weak, and strong shading is considered. The schematic of 4S PV array with bypass and blocking diode is shown in Fig. 2. Bypass and blocking diodes are present to protect the panels and array against "hotspots" and "current reversal" [28], [29]. Further, panels when uniformly illuminated, i.e., at zero shading condition, the *I--V* curves of the individual panel sums up and forms a single peak in *P–V* curve. Moreover, due to the fixed position of the panels and nonuniform irradiation across the panels, introduces the steps in *I–V* curve and in-turn creates multiple peaks in a *P–V* curve. Depending on the strength of shade, less or more power peaks occur in *P–V* characteristics. To make it clear, *I–V* and *P–V* curve that corresponds to zero, weak, and strong shade pattern are shown in Fig. 3(a) and (b) with local (LMPP) and global (GMPP) power peaks are highlighted in different color. Due to the existence of multiple peaks in a *P–V* curve, a suitable MPPT method which has the inherent ability to track the global peak even under fluctuating weather conditions should be employed. It is noteworthy to mention that the efficiency of the adopted MPPT algorithm affects the overall efficiency of PV system as well. Hence, by considering all the above facts, a novel FPA algorithm is proposed to design an MPPT controller, which tracks the global peak irrespective of atmospheric conditions. Proper care is taken while designing to ensure that global maximum power is tracked under all possible dynamic irradiated conditions.

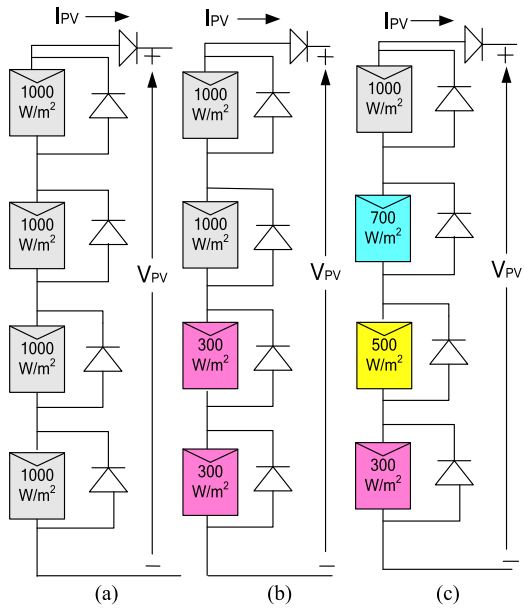


Fig. 2. String of four panels in series (4S) with respective test cases Case(a): Zero shading—Pattern 1, Case(b): Weak shading—Pattern 2. (c): Strong shading—Pattern 3.

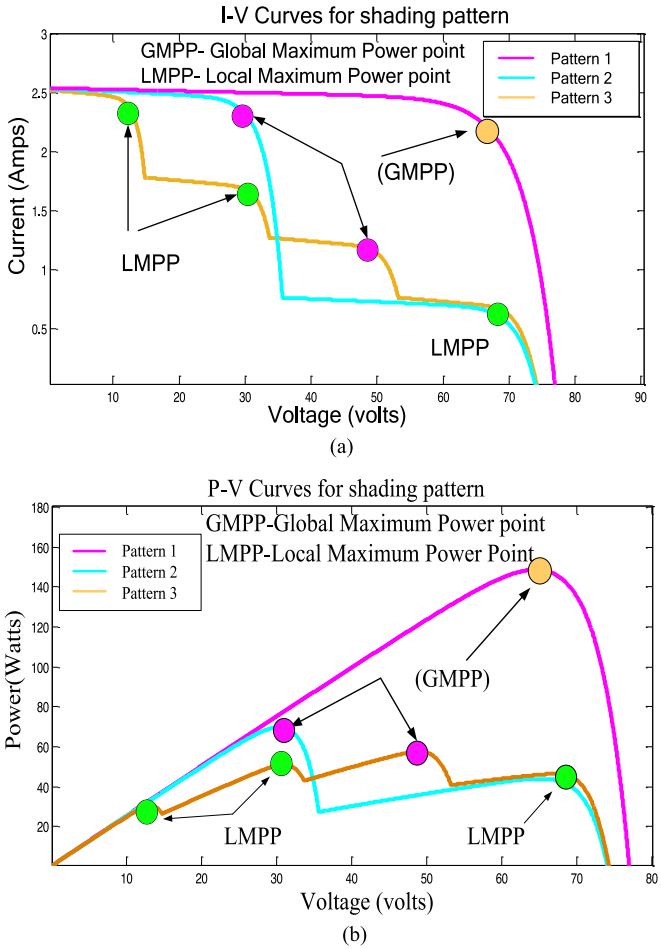


Fig. 3. (a) *I–V* curves corresponding to different shade patterns. (b) *P–V* curves corresponding to different shade patterns.

### B. Flower Pollination Algorithm

Inspired by the natural pollination process in flowers, FPA was first proposed by Xie Yang in 2012 [34]. Pollination is a phenomenon that refers to transfer of pollens from one species to the other. The term pollination is arrived either by cross pollination or self-pollination. This process helps the flowers to emerge new species. Based on pollens, two types of pollination occur: 1) abiotic process—self-pollination—species of same type, i.e., pollens of the same plants, fertilize to emerge new species where wind is the pollinating agent; 2) biotic process—cross pollination—transfer of pollens takes place between two different species where the pollinators are honey bees, bats, and birds. Here, it is noteworthy to mention that in FPA, 90% of pollination is cross pollination and remaining 10% is self-pollination [34]. The control between cross and self-pollination is restricted by a probability switch $P \in [0, 1]$. Flower constancy is measured by reproduction probability where it is directly proportional to flowers involved in pollination. To implement FPA, the fundamental design rules followed are

*Rule 1:* Biotic or cross pollination represents a global pollination process and follows levy flight for transfer of pollens. For instance, the *i*th pollen on *k*th iteration updated via biotic pollination given in [34] can be expressed as

$$x_i^{k+1} = x_i^k + L(\mathrm{gbest} - x_i^k) \tag{4}$$

where "gbest" refers the current best solution obtained with a set of pollens ($x_i^k$). "$L$" is the levy factor responsible for the transfer of pollens. Further, it is a key parameter that strengthens the pollination process. Since the pollen transfer follows the Levy distribution, the flight of the pollen in levy distribution presented in [34] is given by

$$L = \frac{\lambda\Gamma(\lambda)\sin(\pi\lambda/2)}{\pi}\frac{1}{S^{1+\lambda}}(S >> S^0 > 0) \tag{5}$$

where "$\Gamma(\lambda)$" is the standard gamma function and the distribution is applicable to a large step size which is greater than zero ($S >> S^0 > 0$). Based on trial and error method the authors have arrived the value of "$\lambda = 1.5$" to ensure faster convergence.

*Rule 2:* Abiotic or self-pollination is characterized by the local pollination process. The characteristic equation for local pollination is given as follows

$$x_i^{k+1} = x_i^k + \varepsilon(x_m^k - x_j^k) \tag{6}$$

where "$x_m^k$" and "$x_j^k$" are different pollens, i.e., flowers of the same species. The term "$\varepsilon$" (epsilon) represents the local search in distribution $\varepsilon \in$[0, 1]. Local pollination occurs in neighborhood of flowers that are at shorter distance, whereas global pollination happens with plants at elongated distance. Thus, to control the switching between pollination process probability switch "$P \in [0, 1]$" is used. In most of the cases, the probability switch ($P$) is kept at optimal value of 0.8.

Since the FPA algorithm follows only two processes, i.e., cross and global pollination, it is very much desirable to apply this method for solving nonlinear optimization problems [34]. Moreover, this method is best suited for MPPT applications since, it explores globally and exploits locally within a single iteration. The best part of the algorithm is, unlike other bio-inspired algorithm, this FPA introduces randomness in every iteration via self-pollination. To date, no such algorithm with both the features in single-stage process has evolved. Instead, earlier algorithms are developed by fusing the properties of two different algorithms [33]. In such cases, the inevitability of parameter tuning of either algorithm or steps for implementation increase the complexity of the method.

### C. FPA Implemented for MPPT Application

FPA is a new class of nature inspired algorithm. The steps involved in implementation of the FPA method in MPPT application are devised and are explained as follows:
*Step 1: Initialization of Parameters*: Maximum iteration number (*N*), limits on duty cycle ($X_{\min}$and$X_{\max}$), probability switch ($P$) and initial duty cycle population size ($X_1$, $X_2$, $X_3$, $X_4$ , and $X_5$) are set to 25, 0.1, 0.9,0.8, and 5, respectively.
*Step 2: Fitness Evaluation*: In this step, pollens suitability is evaluated by using fitness function. For demonstration, the evaluated fitness, i.e., quality of pollens position is indicated with the help of stars in Fig. 4(b).
*Step 3: Pollination Process:* According to Fig. 4(b), pollen ($X_4$) with higher fitness is marked as gbest. A random number between 0<rand<1 is generated based on probability switch ($P$) and the condition *(if rand>P)* every pollen in the pool must undergo either cross or self-pollination.

1) *Cross Pollination*: In the present case, it is assumed that four particles undergo cross pollination and the remaining one pollen follows self (or) local pollination. The resultant trajectory (OC) showing the movement of pollen ($X_1$) toward GMPP is arrived by interaction between vector (OA) showing gbest and levy factor vector (OB), i.e., $L(\mathrm{gbest} - x_i^k)$.
2) *Self-Pollination:* With one pollen ($X_3$) undergoing local pollination in the first iteration, its position updation for next iteration is explained in Fig. 4(d). Since the local pollination happens between the pollens of same species, pollens $X_2$ (vector OA') and $X_5$ (vector OB') have attributed to arrive at new position via vector OC'.

*Step 4: Pollens New Position*: Following Step 3, all the pollens in the pool arrive at their new position (i.e., duty cycle) via cross or self-pollination is represented in Fig. 4(e).
*Step 5: Termination Criterion:* Repeat the steps between 2 and 5 until all the pollens converge to reach the maximum power for the given iteration count, i.e., $N = 25$.
*Step 6: Reinitiating Search on Insolation Changes:* To identify the occurrence of partial shading condition/irradiation change, threshold changes in voltage and current values between iterations are monitored. Based on the change in threshold values, the irradiation change is noted and the algorithm gets reinitialized with the search process restarts from Step 1. To perceive threshold limits, the authors have performed numerous experimentations with large and small irradiation changes.

From the experiments based on the trial and error method, the optimum values of threshold limits are arrived as 0.2 and 0.1 for

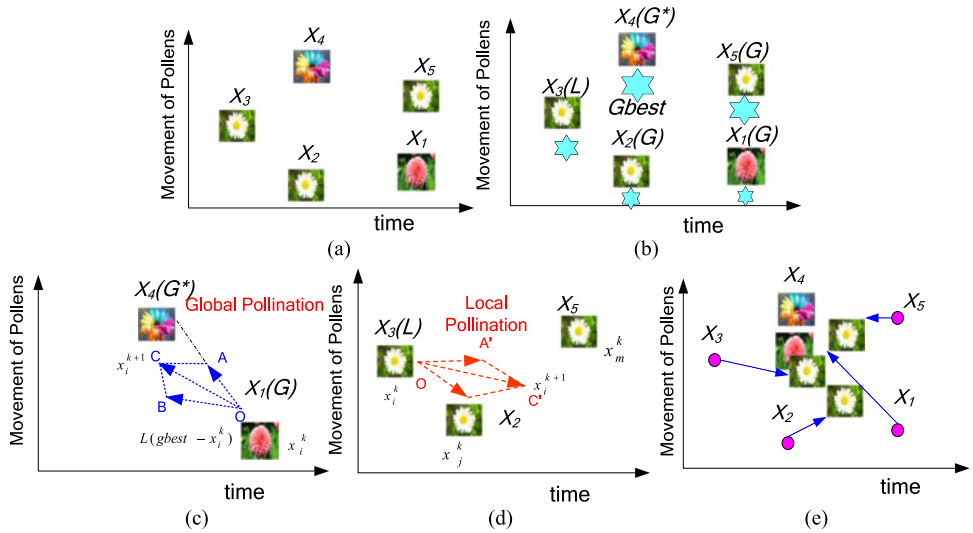


Fig. 4. Updation of the pollen position via FPA method. (a) Initialization of pollens. (b) Fitness function evaluation. (c) Cross pollination step. (d) Self-pollination step. (e) Duty cycle updation for the next iteration.

voltage and current values, respectively. Moreover, the values arrived are in agreement with those seen in the literature [25], [28]. Thus, the occurrence of IC can be detected by checking the following condition

$$\frac{V_{\mathrm{PV}}(k) - V_{\mathrm{PV}}(k-1)}{V_{\mathrm{PV}}(k)} \geq 0.2 \tag{8}$$

$$\frac{I_{\mathrm{PV}}(k) - I_{\mathrm{PV}}(k-1)}{I_{\mathrm{PV}}(k)} \geq 0.1 \tag{9}$$

where "$V_{\mathrm{PV}}(k)$" is the PV voltage at $k$th iteration, "$V_{\mathrm{PV}}(k-1)$" is the PV voltage in the previous iteration, "$I_{\mathrm{PV}}(k)$" is the PV current at $k$th iteration and "$I_{\mathrm{PV}}(k-1)$" PV current at the previous iteration.

## IV. Simulation Results

To evaluate the FPA performance and its suitability to MPPT application, three different shade pattern as discussed in Section II with four PV panels connected in a string is tested. Additional tests such as one step and two step change in irradiation have also been investigated. Further, analysis on the duty cycle convergence of optimal value has been exclusively illustrated with the help of *P–V* curves. Based on the simulated results, a quantitative comparison is made between FPA, PSO, and P&O methods in terms of efficiency and convergence time. For simulation, the algorithms developed in MATLAB platform are tested with the system configuration of 500-GB memory, 4-GB RAM and Intel i7 Processor. The algorithms (FPA, PSO, and P&O) considered for the study are carefully coded and their parameters are carefully tuned so as to exhibit similar performance. It is noteworthy to mention that both PSO and FPA method follow five random duty cycle initialization. The proposed MPPT control structure with dc–dc boost converter is shown in Fig. 5. The sampling time between duty cycles is taken as 0.03 s. Generally, parameter tuning is one of the essential stipulations that decide the performance of bio inspired algorithms.

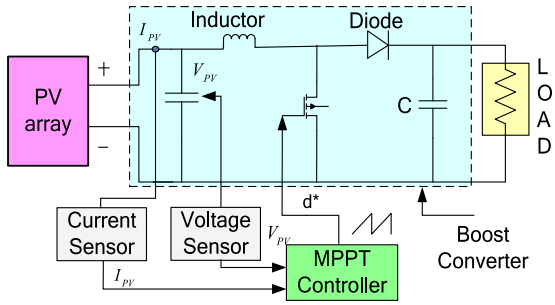


Fig. 5. System structure with MPPT controller.

TABLE I
Parameters of PSO, FPA, & P&O Method

| PSO | FPA | P&O |
|---|---|---|
| $C_1 = 1.4$ | $P = 0.8$ | $D = 0.75$ |
| $C_{1\min} = 1$ | $\gamma = 1.5$ | $\Delta D = 0.005$ |
| $C_2 = 1.8$ | – | – |
| $C_{2\min} = 1$ | – | – |
| $W_{\max} = 0.3$ | – | – |
| $W_{\min} = 1$ | – | – |

Further, it is an important factor in achieving faster convergence toward GMPP. Hence, in this paper, two parameters of FPA 1) probability switch (P) and 2) scaling factor ($\gamma$), six parameters of PSO: velocity limits—($C_1, C_{1\,\min}, C_2,$ and$C_{2\,\min}$) and inertia weights ($W_{\min}$and$W_{\max}$), two parameters of P&O: change in duty ($\Delta D$) and initial duty ($D$) are tuned with extreme care optimal performance. The values arrived for each method is presented in Table I.

### A. Case (a)—Zero Shading—(Pattern 1)

The MPPT curves under uniform irradiation, i.e., zero shading—case-(a)—pattern 1 illustrated in Fig. 2 employing P&O, PSO, and FPA are portrayed in Fig. 6(a). Since there

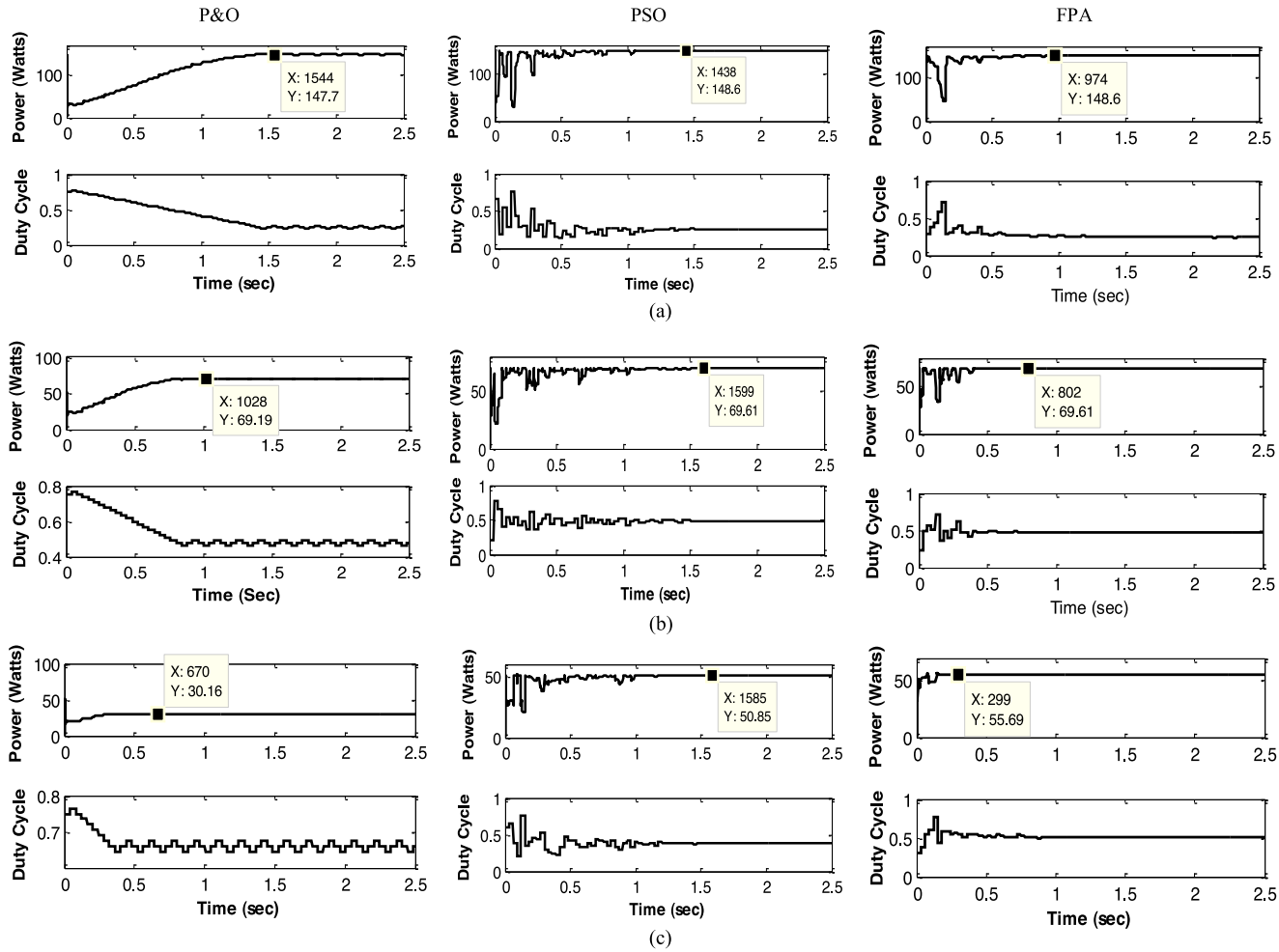


Fig. 6. (a) Simulated power and duty cycle curves of P&O, PSO, and FPA method for zero shading—Case(a)—Pattern 1. (b) Simulated power and duty cycle curves of P&O, PSO, and FPA for weak shading—Case(b)—Pattern 2. (c) Simulated power and duty cycle curves of P&O, PSO, and FPA for strong shading—Case(c)—Pattern 3.

exists a single peak at 148.6 W, reaching peak in this case is a simple task for all the three methods. However, the results analysis is quite useful in terms of knowing the tracking speed and time taken by the algorithm to converge. From the results, it can be seen that both PSO and P&O method took 1.5 and 1.2 s, respectively, to converge, whereas FPA method reaches to a global peak within 0.5 s. Further, it is interesting to note that FPA locates the optimized position in quick time, i.e., converges after second iteration. It is noteworthy to mention that P&O convergence purely depends on its initial value [2], [11].

### *B. Case (b)—Weak Shading—(Pattern 2)*

The power and duty cycle curve that corresponds to the weak shading—case (b)—pattern 2 illustrated in Fig. 2 is shown in Fig. 6(b). In this case, FPA converges to GMPP of 69.61 W in less than 0.5 s, whereas PSO takes 1.5 s to converge at GMPP. Even though PSO method senses GMPP in first iteration larger velocity created during position updation slows down its convergence speed and increases the iteration count. Surprisingly, P&O method located GMPP in this case due to proper duty cycle initialization made on left side of MPP, i.e., global peak side. However, the time taken is quite larger due to its fixed step size. Moreover, there is always a possibility for P&O to settle at a local peak when it is wrongly initialized.

### *C. Case (c)—Strong Shading—(Pattern 3)*

The performance of the MPPT method can be critically analyzed when strong shade occurs due to exposure of more number of panels to different irradiation. This condition is realized in case (c)—strong shading—pattern 3 shown in Fig. 2(c). The shade in this case has led to have four different peaks with three LMPP occurring at 30, 51, and 49 W, respectively, and one GMPP at 55.7 W. The power and duty cycle curve corresponding to this case is illustrated in Fig. 6(c). The graphs indicate that both PSO and P&O method are able to settle only at local peak (LMPP), whereas FPA successfully reach GMPP in minimal time. For better understanding, the process involved in reaching GMPP with FPA method is elaborated further with the help of Fig. 7.

Assumed with five random initial duty cycles ($X_1$, $X_2$, $X_3$, $X_4$, and $X_5$) spread over the entire *P–V* curve shown in Fig. 7(a). In the first step, FPA method evaluates

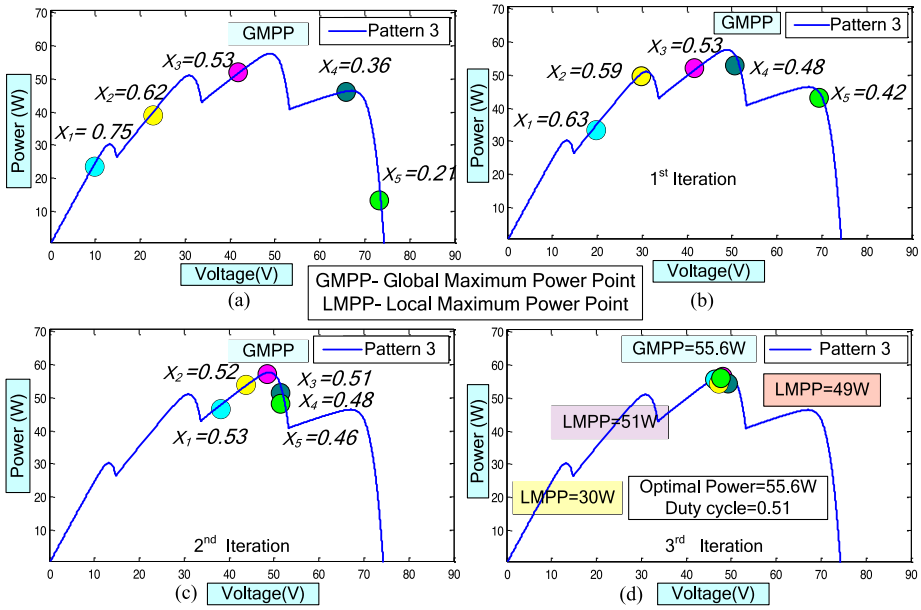


Fig. 7. (a) Initialization of pollens on a PV curve. (b) Movement of pollens after first iteration. (c) Realizing global point peak in third iteration. (d) All pollens reaching global peak.

the goodness of the solution via fitness function for all the five duty cycles. After evaluation, one optimal duty cycle corresponding to maximum power is located, say at $X_3 = 0.53$ for instance. Once the fitness corresponding to all duty cycles, i.e., pollens are evaluated. The method guides the pollens to undergo either cross (or) self-pollination determined by probability switch ($P$). In the present case, during first iteration pollens ($X_1$, $X_3$, $X_4$, and $X_5$) undergoes cross pollination and the remaining pollen ($X_2$) follow self-pollination to arrive their new position for the next iteration. At the end of first iteration, the location of GMPP has shifted from $X_3 = 0.53$ (third pollen) to $X_4 = 0.48$ (fourth pollen) following global pollination. Keeping the new pollens position as reference (GMPP), the duty cycle, i.e., pollens position, are updated via further iterations. Once FPA method recognizes the MPP at the end of the second iteration ($X_3 = 0.51$) as shown in Fig. 7(c), FPA method converges faster to an optimal point in further iterations and reach global peak faster as shown in Fig. 7(d). On the other hand, while looking at the search process of PSO method, the particle (duty cycle) with the highest power attracts the remaining particle to converge toward it. This search process does not guarantee local search in every iteration. Moreover, velocity updation comes to halt when all the particles get closer to the best solution. Hence, there is no scope to introduce randomness in the control variable (duty cycle). This characteristic in FPA method enables to be highly suitable for MPPT application. Therefore, from the above, it is understood that depending on the fitness of pollens and probability switch, the programmed FPA method in every iteration will guide the pollens toward global search or local search.

Similar analysis is further extended with respect to duty cycle variation on a time scale as shown in Fig. 8, justifies the performance of the FPA method in reaching global MPP. Variation in duty cycle convergence validates FPA performance with

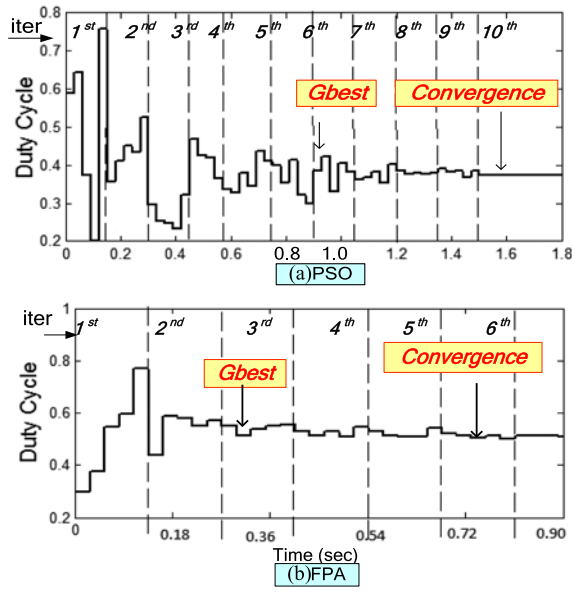


Fig. 8. Duty cycle convergence in (a) PSO and (b) FPA.

small variation in steps. Moreover, both PSO and FPA method have similar scope in reaching GMPP. However, due to absence of randomness in PSO method, it got trapped in local peak at duty $= 0.39$ and it steadily loses its diversity in particles updation. This makes PSO unjustified in finding GMPP under strong shaded condition. Further, the comparison infers that initialization of high velocity makes the duty cycle constantly fluctuating to cost an additional nine more iteration to converge for MPP.

### *D. Step Change in Partial Shading Condition and Irradiation Change*

Different case studies performed earlier illustrates FPA robustness over other MPPT techniques under dynamic irradiated

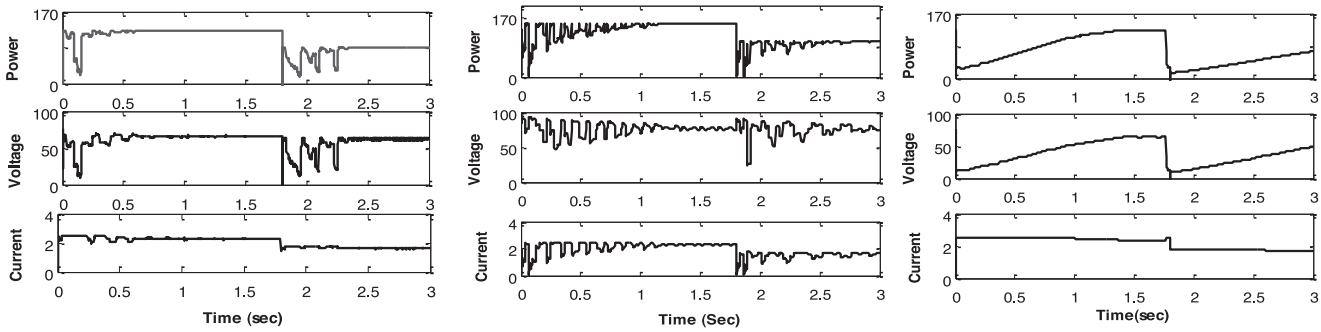


Fig. 9. Simulated curves of P&O, PSO, and FPA for step change under PSC.

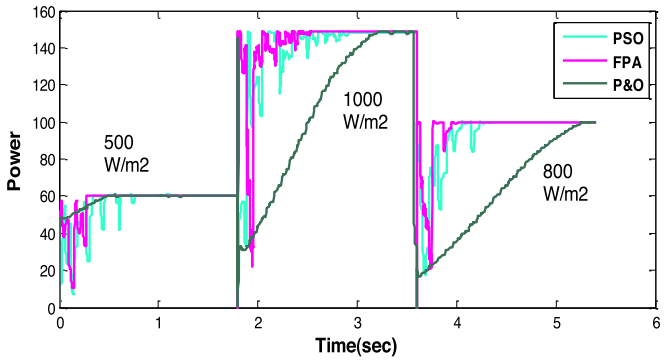


Fig. 10. Convergence characteristic for FPA, PSO, and P&O under change in uniform irradiation condition.

conditions. But in practical situations, PV arrays are often subjected to varying irradiation changes since they are exposed to changing weather conditions. Hence, it becomes mandatory to study the transient behavior of the FPA method under such environmental changes. In this view point, two cases namely 1) a step change from pattern 1 to pattern 2 and 2) three step uniform insolation change cases are studied. The simulated power, voltage, and current curves for both the cases are shown in Figs. 9 and 10. In both cases, whenever there is an occurrence of irradiation change neither due to partial shading nor uniform insolation, duty cycles of PSO and FPA method are reinitialized to track the new GMPP. FPA method experimented for step changes once again prove its proficiency in accomplishing quick convergence at 0.45 s, whereas the PSO strives to reach MPP in both the cases. Although PSO method shows less steady-state oscillations, the time taken to converge and the oscillations present in the system tamper its performance. Both PSO, P&O method has taken 1.3 s for first pattern and 1.2 s for the second pattern, respectively, to reach MPP. In the next case, three step insolation values say 500, 800, and 1000 W/m$^2$ is created at uniform time intervals of 1.8 s. It is accepted from Fig. 10, the FPA method has shown judiciary performance in producing higher efficiency compared to PSO and P&O methods.

Compiling the simulation study results, a critical quantitative analysis based on %efficiency, tracking speed, and attained maximum power is performed for three test patterns and the compiled data are presented in Table II. From the table, it is evident that FPA ranks first position followed by PSO and P&O methods. In all the cases, the FPA has shown its top indentation in achieving high quality of results.

## V. Experimental Setup and Validation

To authenticate the simulated findings, a hardware prototype of the proposed system was constructed and tested in the laboratory where a dedicated PV simulator (CHROMA 62050H) is used as a PV source. The MPPT algorithms considered for study are coded and executed by using an Arduino UNO controller. Having two timer circuit arrangements, the controller can support up to 10-kHz frequency. Hardware specifications of dc–dc boost converter with PV panel details are listed in Table III.

Similar to simulation study, experimentation has been carried out for zero, weak, and strong irradiated conditions. In order to achieve similar test results, dc–dc boost converter in hardware is operated in a continuous conduction mode. The output ripple level of the converter is limited to ensure the safety operation of the hardware model. The hardware prototype test setup developed in the laboratory with dc–dc boost converter interfaced with real time PV simulator is shown in Fig. 11. The simulator (chroma-6050S) is utilized to program different shading patterns for experimentation.

It is been well understood from the literature review that the swarm optimized PSO method, when started with three duty cycle, it loses its diversity and may end up in LMPP [34], hence to deal with partial shading conditions effectively, numerous trials with different shading patterns have been carried out and the optimal number of duty cycles per iteration is found to be five. To allow the system to reach steady state, sampling interval given in the duty cycle feedback is fixed at 300 ms. The experimental voltage, current, and power waveforms for case (a)—zero shading—pattern 1 is shown in Fig. 12. From the hardware results, it is noticed that FPA has convincingly converged to the global maximum of 145.7 W within 0.6 s, whereas PSO took 1.5 s to attain converge at 143.5 W. Since the shading is absent in this case, the P&O method comfortably reaches to MPP within 1 s. For clarity, power, voltage, and current values attained after reaching steady state are displayed in Fig. 12. Further, three point behavior of P&O method is clearly visible in the presented results.

Alike previous case, PV systems are further tested for the partial shaded condition having two and four peaks. The input

TABLE II
QUANTITATIVE COMPARISON BETWEEN FPA, PSO, AND P&O METHODS IN TERMS OF EFFICIENCY, POWER TRACKED, AND TRACKING TIME

| Shading pattern | Method | Voltage at MPP (V) | Current at MPP (A) | Power at MPP (W) | Rated Power (W) | Efficiency (%) | Time taken reach MPP (s) |
|---|---|---|---|---|---|---|---|
| Case(a) | FPA | 65.1025 | 2.28 | 148.64 | 148.9 | 99.85 | 0.45 |
| | PSO | 65.85 | 2.25 | 148.61 | | 99.81 | 1.05 |
| | P&O | 62.65 | 2.35 | 147.7 | | 99.20 | 1.3 |
| Case(b) | FPA | 30.87 | 2.255 | 69.91 | 69.68 | 99.90 | 0.45 |
| | PSO | 30.7 | 2.24 | 68.81 | | 99.90 | 1.2 |
| | P&O | 31.04 | 2.20 | 69.07 | | 99.12 | 0.75 |
| Case(c) | FPA | 50.37 | 1.12 | 55.71 | 56.61 | 99.21 | 0.60 |
| | PSO | 32.19 | 1.55 | 49.96 | | 86.72 | 1.2 |
| | P&O | 13.75 | 2.15 | 29.68 | | 51.52 | 0.36 |

TABLE III
DESIGN SPECIFICATIONS OF DC–DC BOOST CONVERTER & SHELL S36 PV PANEL

| S.No. | Parameter | Value |
|---|---|---|
| 1 | Switching frequency | 10 kHz |
| 2 | Inductor | 0.5 mH |
| 3 | Capacitor | 450 V, 100 $\mu$F |
| 4 | Load resistance | 10 A, 100 $\Omega$ |
| | Shell S36 Panel details | |
| 1 | Power at MPP $P_{\mathrm{mpp}}$ | 36 W |
| 2 | Power voltage $V_{\mathrm{mpp}}$ | 16.5 V |
| 3 | Open-circuit voltage $V_{\mathrm{oc}}$ | 21.4 V |
| 4 | Short-circuit current $I_{\mathrm{sc}}$ | 2.30 A |

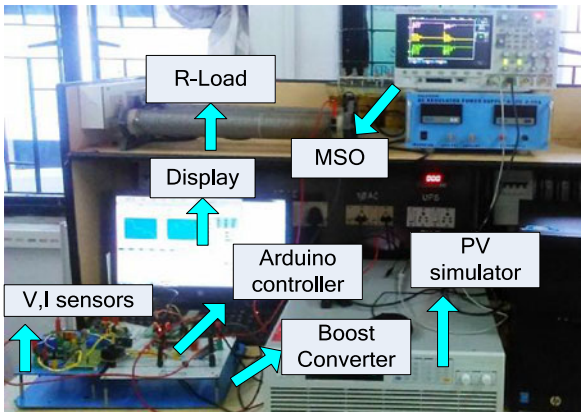


Fig. 11. Hardware prototype model for proposed MPPT scheme.

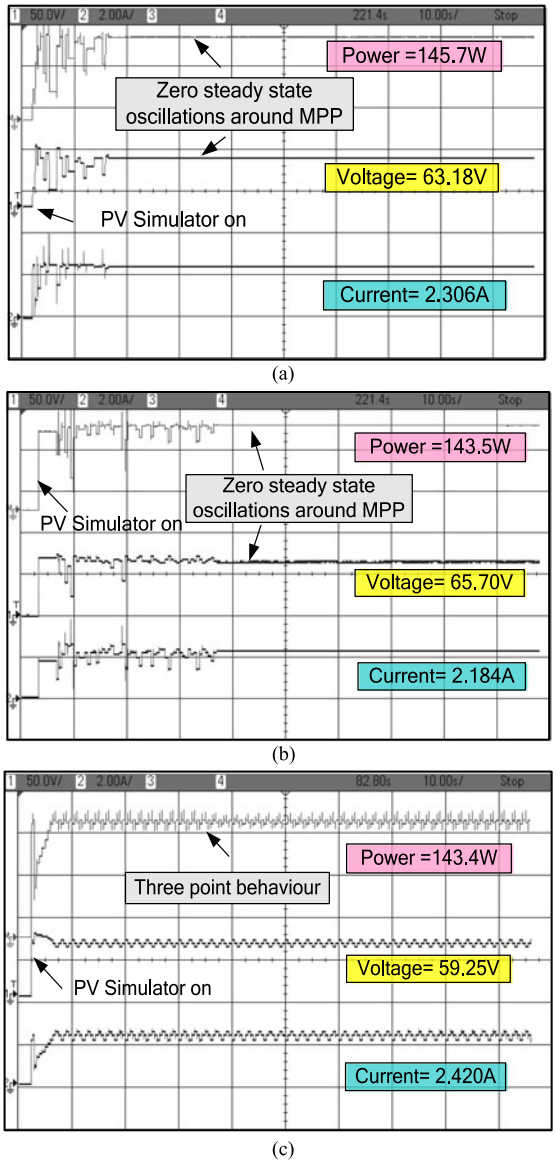


Fig. 12. Hardware realization of P&O, PSO, and FPA for zero shading—Case (a)—Pattern 1. (a) FPA. (b) PSO. (c) P&O.

voltage, current, and power waveforms for PSO, FPA, and P&O for pattern 2 is shown in Fig. 13. From the figure, it is inferred that FPA method quickly recognizes the global peak via its local and global pollination. The algorithm managed to climb the GMPP within 0.6 s. In case of PSO method, it took around 1.25 s to settle at 71.14 W. Since, the initialization of duty cycle starts with 0.75, i.e., on the left side of the *P–V* curve, the P&O gets it peak quickly and reached the global peak at 0.543 of duty cycle. However, if the duty cycle is started on the right side of the *P–V* curve, it is expected to get trapped in local minima.

Yet another case study of multiple peak occurrences is considered to test the robustness of all the three algorithms. Having the benefit of exploration and exploitation, the superior FPA method alike simulation reaches GMPP within 0.45 s. PSO method in resemblance to simulation study got caught in one of the local peaks (LMPP). The drawback of large velocities in duty cycle adds 1.25 s for PSO method to attain its convergence. On the other hand, the P&O method as expected got trapped in one of

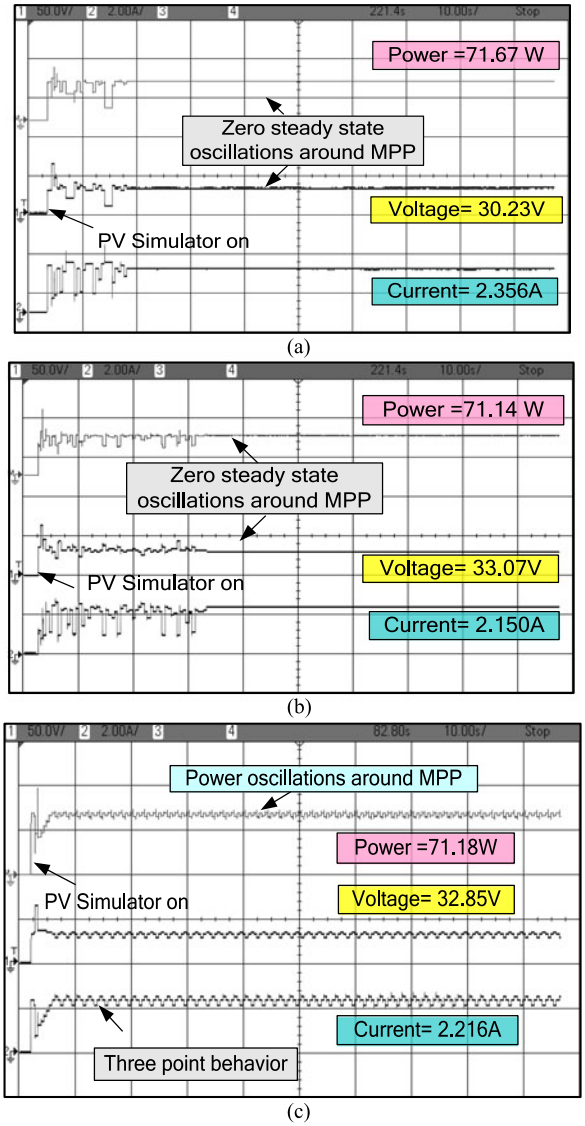


Fig. 13. Hardware results of P&O, PSO, and FPA for weak shading—Case (b)—Pattern 2. (a) FPA. (b) PSO. (c) P&O.

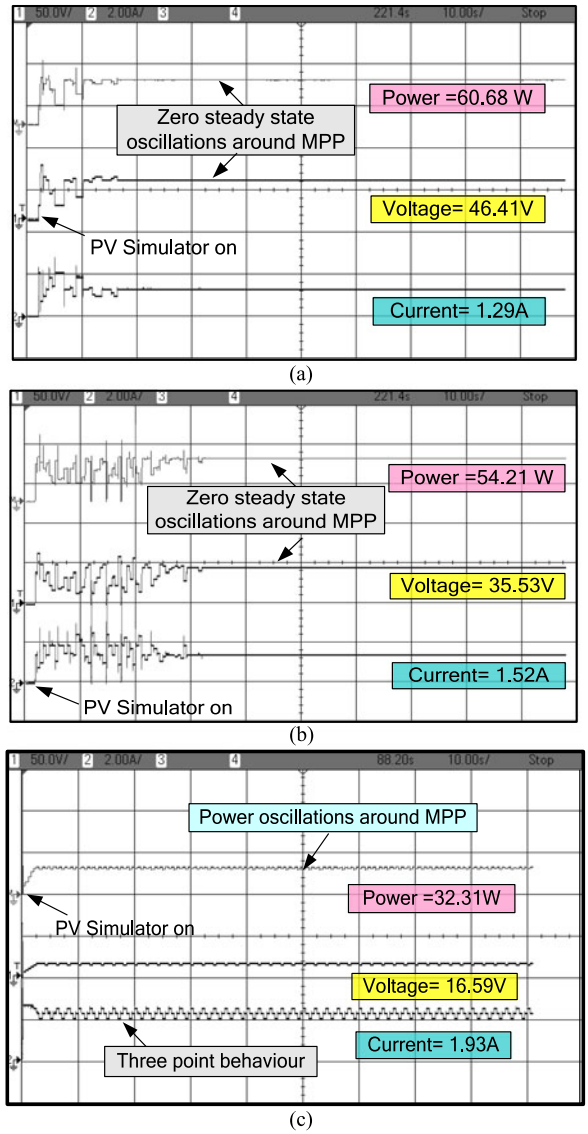


Fig. 14. Hardware results of P&O, PSO, and FPA for strong shading (PSC)—Case (c). (a) FPA. (b) PSO. (c) P&O.

the local peaks at 35.31 W. The hardware realization for P&O, PSO, and FPA are shown in Fig. 14.

In order to demonstrate the method superiority under change in PSC, during experimentation step change from pattern 1 to pattern 2 is experimented via prototype model developed in the laboratory. Each pattern is made to run for an interval of 5 s. During the tracking process, the method continues to check the occurrence of PSC and gets reinitialized when shading occurs. The hardware waveform for step change in shaded condition is illustrated in Fig. 15. The obtained result under irradiation change illustrates that FPA is highly sensitive to detect PSC and it keeps maintaining the credibility of climbing the global peak in quick succession. Although it is a dynamically irradiated partial shadow condition, the PSO algorithm settles at MPP convincingly after a long struggle. But, the convergence time is quite lengthy when compared to FPA. As steady state oscillations around MPP are being highlighted as a major disadvantage, P&O made a unique attempt to reach MPP, and finally settles with three point behavior.

Thus, from the case study, it can be summarized from both simulation and hardware results that novel FPA is highly capable of tracking MPP irrespective of shading pattern created. Moreover, natural simplicity in FPA avoids the demand for the high-end controller. Based on the results obtained, a quantitative analysis is made between methods based on six crucial parameters that influence the selection of method. Six axial pictorial representation that corresponds to steps taken to converge, Tracking speed, switching characteristics, trapping to local peak, oscillations around MPP, and dependency to initial design is utilized to convey the results obtained and it is given in Fig. 16. Owing to the experimentations, the figure presented can be understood in the following way. The uniformity in occupying lesser area in all cases (zero, weak, and strong shading) is an indication of reliable and optimal performance and wider spread

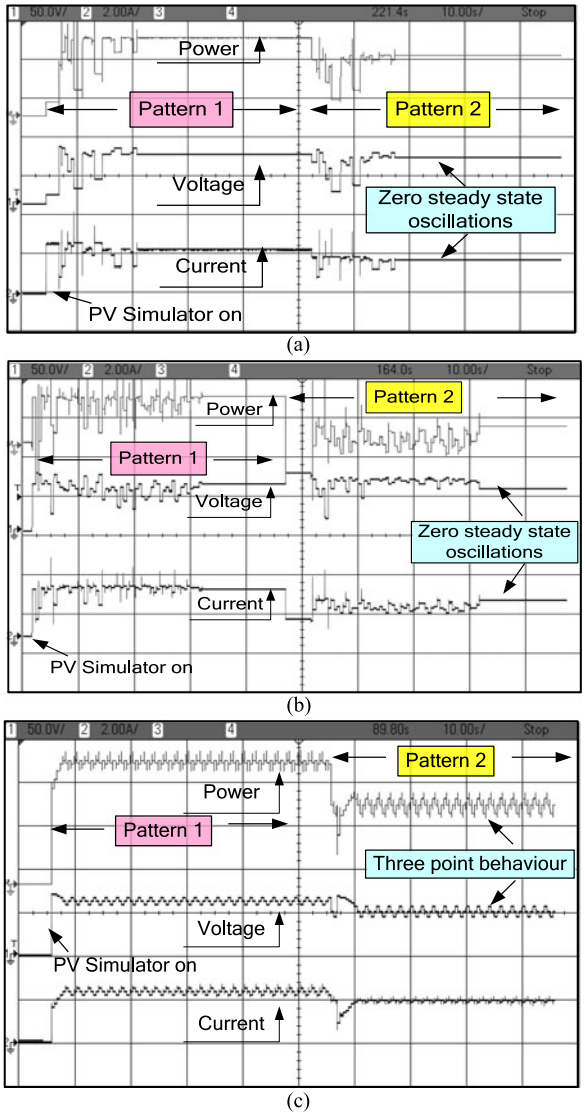


Fig. 15. Hardware results of P&O, PSO, and FPA for occurrence in partial shading condition. (a) FPA. (b) PSO. (c) P&O.

of area is an indication of poor performance, respectively. Thus, FPA method strongly demonstrates its robustness over PSO and conventional P&O methods.

## VI. Comparative Study

Scholarly research work on MPPT can be seen in the last few years. Specifically, new methods have evolved on MPPT applications with possibilities of reaching global peak under partial shaded condition. The impact of green power generation is clearly visible in the recent years with contribution of different methodology proposed for performance enhancement of PV system. To understand the contribution of the FPA method in the field of MPPT application, a comprehensive comparison is carried out between FPA and other methods that are well established in MPPT arena. In particular, the crucial seven parameters that decides the performance of systems is analyzed and based on the study results, a wheel chart is prepared and presented inFig. 17. The chart can be understood in this way, whenever the method occupies lesser area, then, it is an indication of poor performance with respect to seven parameters and vice versa. A closer examination of the chart reveals that FPA satisfies all the requirements and strengthen its wheel area. Further, based on the information presented in the chart, the methods have been ranked in the following order 1) FPA, 2) RSM, 3) PSO, 4) Fuzzy, 5) ANN and conventional methods. A qualitative comparison with many methods is always a handy tool for predicting the method's performance. Hence, a qualitative survey is included between methods based on all possible parameters is presented in Table IV. From the table and wheel chart the following conclusions can be derived, FPA method is 1) robust and reliable, 2) simpler in structure and easy to code and compile, 3) effective to differentiate local and global peaks under PSC, and 4) quick convergence with zero steady-state oscillations.

## VII. Evaluation on Energy Saving

The simulation study supported by hardware realization and comparison with other methods proved the trustworthy nature of FPA algorithm. Although a fair qualitative and quantitative analysis have proved FPA superiority in terms of convergence time, efficiency, and accuracy. A comprehensive comparison on energy yield and energy saving made by each method will further substantiate the potential of the proposed method. Hence, in regard to dynamic change in irradiation and PSC discussed in earlier sections, few more parameters such as energy saved, income generated, and units produced by each method are discussed in detail.

Using the hardware prototype model developed in the laboratory, an economy analysis based on energy saving is performed under real-time situations. For experimentation the 1-kW PV rooftop solar PV installed at Technology Tower building of VIT University, Vellore, is utilized. For computation, the effective sun hours are taken at 6 h and operated between 10 A.M.–4 P.M. at 30 °C. To evaluate the system quantitatively, PV plant of 1-kW capacity is exposed to six different shading patterns in a day. The numerically simulated *P–V* curve pattern for different shade is plotted in Fig. 18. With each pattern running for an hour, the net energy yield from morning 10 A.M. to evening 4 P.M. is continuously monitored for each of the algorithms. From the observations, a detailed comparison on net energy yield and income generation is presented in Table V.

Evaluation in Table V clearly notifies that FPA method converged to a global peak (GMPP) maximum number of times, whereas the PSO and P&O methods got trapped in local peaks (LMPP). This change has created an impact in net energy yield of the individual methods. Among the total energy generated by individuals, FPA has emerged to top of the list by generating 3.82 units per day and PSO at second spot by generating 3.58 units per day. Based on the number of units produced per day, the income generated in a year is arrived. Albeit the income generated between FPA and PSO has negligible difference, it will vary in wider extent when the plant is scaled up to larger power ratings. From the study performed, the common parameters that influence FPA to achieve high energy yield are tracking speed and accuracy. With utmost simplicity and ease of

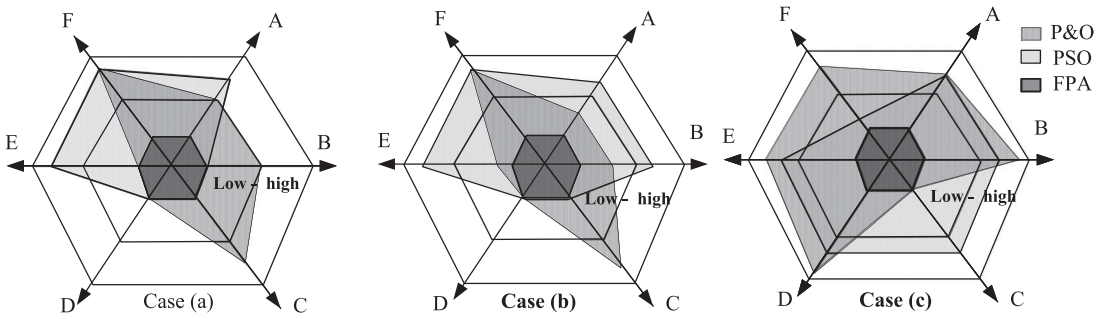


**A-**Steps to attain Convergence, **B-**Tracking Speed, **C-**Switching Transients, **D** -Trapping To Local Peak, **E-**Oscillations around MPP, **F-** Dependency to the initial design

Fig. 16. Six-axial pictorial representation of parameters governing the performance of MPPT method in the order low–high.

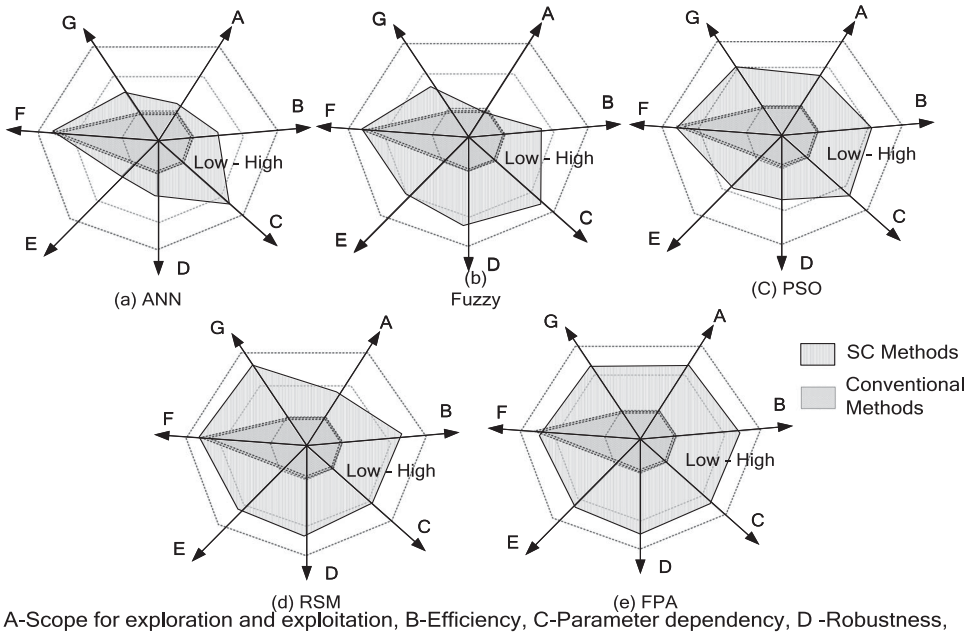


A-Scope for exploration and exploitation, B-Efficiency, C-Parameter dependency, D -Robustness, E-ability to track under PSC, F- Ability to track under normal operating conditions G-Panel independancy

Fig. 17. Seven-axial representation of parameters affecting the performance of various SC techniques.

TABLE IV
PERFORMANCE COMPARISON OF VARIOUS MPPT TECHNIQUES

| S.No. | Parameter | P&O [9] | Fuzzy [19] | PSO [24] | DEPSO [33] | RSM [29] | FPA |
|---|---|---|---|---|---|---|---|
| 1 | Steady-state oscillation | Large | Less | Zero | Zero | Zero | Zero |
| 2 | Tracking speed | Slow | Moderate | Moderate | Fast | Fast | Fast |
| 3 | Complexity | Less | Moderate | High | High | Less | Less |
| 4 | Procedural complexity | Less | Moderate | Moderate | Large | Less | Less |
| 5 | Memory requirement | Less | Large | Less | High | Less | Less |
| 6 | Computational complexity | Less | Large | Moderate | High | Less | Less |
| 7 | Performance under PSC | Trapped in LMPP | Less | Moderate | High | High | High |
| 8 | Exploration process | – | – | √ | √ | √ | √ |
| 9 | Exploitation process | – | – | – | √ | – | √ |
| 10 | Execution time | Slow | Moderate | Moderate | Fast | Fast | Fast |
| 11 | Panel dependency | Dependent | Dependent | Independent | Independent | Independent | Independent |
| 12 | Steps involved | 2 | 4 | 4 | 6 | 3 | 2 |
| 13 | Efficiency | Less-under PSC | Less-under PSC | High | High | High | High |

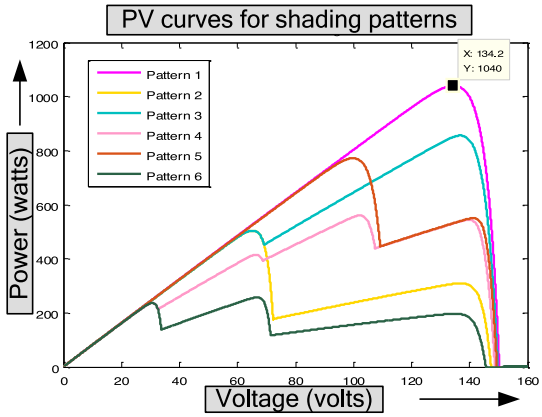


Fig. 18. *P–V* curve corresponding to 6 different shading patterns.

TABLE V
ECONOMICAL ASSESSMENT OF FPA, PSO, AND P&O METHODS

| Method/cases | Energy generated in W·h | | | Units generated | | |
|---|---|---|---|---|---|---|
| | FPA | PSO | P&O | FPA | PSO | P&O |
| Pattern 1 for 10–11 A.M. | 1040 | 1036 | 1038 | 1.00 | 1.00 | 1.00 |
| Pattern 2 for 11–12 noon | 504 | 504 | 502 | 0.48 | 0.48 | 0.48 |
| Pattern 3 for 12–1 P.M. | 856 | 855 | 855 | 0.82 | 0.82 | 0.82 |
| Pattern 4 for 1–2 P.M. | 560 | 550 | 415 | 0.54 | 0.53 | 0.40 |
| Pattern 5 for 2–3 P.M. | 772 | 550 | 503 | 0.74 | 0.53 | 0.48 |
| Pattern 6 for 3 to 4 PM | 236 | 222 | 221 | 0.23 | 0.21 | 0.21 |
| Net Energy Generated in a day | 3969 | 3718 | 3535 | 3.82 | 3.58 | 3.40 |
| Net Energy Generated in a year | 1 448 831 | 1 357 106 | 1 290 348 | 1393 | 1305 | 1241 |
| Total Income generated at INR 15/unit | | | | **20 896** | **19 573** | **18 610** |

implementation, FPA yet another time has outperformed PSO and P&O method, which clearly shows its supremacy for MPPT applications.

## VIII. CONCLUSION

In this paper, a new FPA method for global maximum power tracking isproposed. Various simulations and experimentation have been performed with different case study and test cases. From the simulation and hardware study performed, the following conclusions are arrived:

1) The FPA-MPPT stands unique in MPPT research because, the updation of duty cycle on every iteration is performed via cross or local pollination leading to quick convergence with high accuracy.
2) Simulation studies performed with three different shaded conditions demonstrate that irrespective of shade conditions, FPA method has the ability to differentiate local and global peak. Further, a qualitative study based on different irradiation conditions compared in Section VI ranks FPA to first position followed by RSM, PSO, Fuzzy, ANN, and conventional methods.
3) Economy study on energy savings performed with 1-kW PV system showcase the supreme superiority of FPA algorithm over swarm optimization and conventional methods. Hence, FPA-MPPT is considered to be a suitable technique for MPPT applications over other bio-inspired techniques.

## ACKNOWLEDGMENT

The authors would like to thank the management, VIT University, Vellore, India, for providing the support to carry out research work. This work is carried out at Solar Energy Research Cell, School of Electrical Engineering, VIT University, Vellore. Further, the authors also would like to thank the reviewers for their valuable comments and recommendations to improve the quality of the paper.

## REFERENCES

[1] J. D. Bastidas-Rodriguez, E. Franco, G. Petrone, C. A. Ramos-Paja, and G. Spagnuolo, "Maximum power point tracking architectures for photovoltaic systems in mismatching conditions: A review," *IET Power Electron.*, vol. 7, no. 6, pp. 1396–1413, Jan. 2014.
[2] J. P. Ram, T. S. Babu, and N. Rajasekar, "A comprehensive review on solar PV maximum power point tracking techniques," *Renewable Sustain. Energy Rev.*, vol. 67, pp. 826–47, Jan. 2017.
[3] A. Stojcevski, N. A. Rahim, K. Chaniago, and J. Selvaraj, "Single-phase seven-level grid-connected inverter for photovoltaic system," *IEEE Trans. Ind. Electron.*, vol. 58, no. 6, pp. 2435–2443, Jun. 2011.
[4] R. Bruendlinger *et al.*, "Maximum power point tracking performance under partially shaded PV array conditions," in *Proc. 21st Eur. Photovolt. Sol. Energy Conf. Exhib.*, Germany, 2006, pp. 2157–60.
[5] M. G. Villalva and J. R. Gazoli, "Comprehensive approach to modelling and simulation of photovoltaic arrays," *IEEE Trans. Power Electron.*, vol. 24, no. 5, pp. 1198–1208, May 2009.
[6] S. Shongwe and M. Hanif, "Comparative analysis of different single-diode PV modeling methods," *IEEE J. Photovolt.*, vol. 5, no. 3, pp. 938–946, May 2015.
[7] N. Rajasekar, K. K. Neeraja, and R. Venugopalan, "Bacterial foraging algorithm based solar PV parameter estimation," *Sol. Energy*, vol. 97, pp. 255–265, Nov. 2013.
[8] A. Koran, T. LaBella, and J.-S. Lai, "High efficiency photovoltaic source simulator with fast response time for solar power conditioning systems evaluation," *IEEE Trans. Power Electron.*, vol. 29, no. 3, pp. 1285–1296, Mar. 2014.
[9] M. A. Elgendy, B. Zahawi, and D. J. Atkinson, "Assessment of perturb and observe MPPT algorithm implementation techniques for PV pumping applications," *IEEE Trans. Sustain. Energy*, vol. 3, no. 1, pp. 21–33, Dec. 2011.
[10] A. K. Abdelsalam, A. M. Massoud, S. Ahmed, P. N. Enjeti, "High-performance adaptive perturb and observe MPPT technique for photovoltaic-based microgrids," *IEEE Trans. Power Electron.*, vol. 26, no. 4, pp. 1010–1021, Apr. 2011.
[11] M. A. Elgendy, B. Zahawi, and D. J. Atkinson, "Operating characteristics of the P&O algorithm at high perturbation frequencies for standalone PV systems," *IEEE Trans. Energy Convers.*, vol. 30, no. 1, pp. 189–198, Mar. 2015.
[12] A. Safari and S. Mekhilef, "Simulation and hardware implementation of incremental conductance MPPT with direct control method using Cuk converter," *IEEE Trans. Ind. Electron.*, vol. 58, no. 4, pp. 1154–1161, Apr. 2011.
[13] G.-C. Hsieh, H.-I. Hsieh, C.-Y. Tsai, and C.-H. Wang, "Photovoltaic power-increment-aided incremental-conductance MPPT with two-phased tracking," *IEEE Trans. Power Electron.*, vol. 28, no. 6, pp. 2895–2911, Dec. 2012.
[14] H. A. Sher, A. F. Murtaza, A. Noman, K. E. Addoweesh, K. Al-Haddad, and M. Chiaberge, "A new sensorless hybrid MPPT algorithm based on fractional short-circuit current measurement and P&O MPPT," *IEEE Trans. Sustain. Energy*, vol. 6, no. 4, pp. 1426–1434, Oct. 2015.
[15] J. H. R. Enslin, M. S. Wolf, D. B. Snyman, W. Swiegers, "Integrated photovoltaic maximum power point tracking converter," *IEEE Trans. Ind. Electron.*, vol. 44, no. 6, pp. 769–773, Dec. 1997.
[16] T. Esram, J. W. Kimball, P. T. Krein, P. L. Chapman, and P. Midya, "Dynamic maximum power point tracking of photovoltaic arrays using ripple correlation control," *IEEE Trans. Power Electron.*, vol. 21, no. 5, pp. 1282–1291, Sep. 2006.

[17] N. Femia, G. Petrone, G. Spagnuolo, and M. Vitelli, "A technique for improving P&O MPPT performances of double-stage grid-connected photovoltaic systems," *IEEE Trans. Ind. Electron.*, vol. 56, no. 11, pp. 3456–3467, Nov. 2009.
[18] T. L. Nguyen and K. S. Low, "A global maximum power point tracking scheme employing DIRECT search algorithm for photovoltaic systems," *IEEE Trans. Ind. Electron.*, vol. 57, no. 10, pp. 4473–4482, Sep. 2010.
[19] C.-S. Chiu and T.-S. Fuzzy, "Maximum power point tracking control of solar power generation systems," *IEEE Trans. Energy Convers.*, vol. 25, no. 4, pp. 1123–1132, Nov. 2010.
[20] E. Syafaruddin and K. T. Hiyama, "Artificial neural network-polar coordinated fuzzy controller based maximum power point tracking control under partially shaded conditions," *IET Renewable Power Gener.*, vol. 3, no. 2, pp. 239–253, May 2009.
[21] S. Daraban, D. Petreus, and C. Morel, "A novel MPPT (maximum power point tracking) algorithm based on a modified genetic algorithm specialized on tracking the global maximum power point in photovoltaic systems affected by partial shading," *Energy*, vol. 74, pp. 374–388, Sep. 2014.
[22] L. M. Elobaid, A. K. Abdelsalam, and E. E. Zakzouk, "Artificial neural network-based photovoltaic maximum power point tracking techniques: A survey," *IET Renewable Power Gener.*, vol. 9, no. 8, pp. 1043–1063, Nov. 2015.
[23] M. Miyatake and M. Veerachary, "Maximum power point tracking of multiple photovoltaic arrays: A PSO approach," *IEEE Trans. Aerosp. Electron. Syst.*, vol. 47, no. 1, pp. 367–380, Jan. 2011.
[24] K. Ishaque and Z. Salam, "An improved particle swarm optimization (PSO)—Based MPPT for PV with reduced steady-state oscillation," *IEEE Trans. Power Electron.*, vol. 27, no. 8, pp. 3627–3638, Jan. 2012.
[25] K. Ishaque and Z. Salam, "A deterministic particle swarm optimization maximum power point tracker for photovoltaic system under partial shading condition," *IEEE Trans. Ind. Electron.*, vol. 60, no. 8, pp. 3195–3206, Aug. 2013.
[26] T. S. Babu, N. Rajasekar, and K. Sangeetha, "Modified particle swarm optimization technique based maximum power point tracking for uniform and under partial shading condition," *Appl. Soft Comput.*, vol. 34, pp. 613–624, May 2015.
[27] J. Ahmed and Z. Salam, "A maximum power point tracking (MPPT) for PV system using Cuckoo search with partial shading capability," *Appl. Energy*, vol. 119, pp. 118–130, Jan. 2014.
[28] K. Sundareswaran, S. Peddapati, and S. Palani, "MPPT of PV systems under partial shaded conditions through a colony of flashing fireflies," *IEEE Trans. Energy Convers.*, vol. 29, no. 2, pp. 1–10, Jun. 2014.
[29] K. Sundareswaran, S. Peddapati, and S. Palani, "Application of random search method for maximum power point tracking in partially shaded photovoltaic systems," *IET Renewable Power Gener.*, vol. 8, no. 6, pp. 670–678, Aug. 2014.
[30] K. Sundareswaran, P. Sankar, P. S. R. Nayak, S. P. Simon, and S. Palani, "Enhanced energy output from a PV system under partial shaded conditions through artificial Bee colony," *IEEE Trans. Sustain. Energy*, vol. 6, no. 1, pp. 198–209, Jan. 2015.
[31] K. Sundareswaran, V. Vigneshkumar, P. Sankar, S. P. Simon, P. S. R. Nayak, and S. Palani, "Development of an improved P&O algorithm assisted through a colony of foraging ants for MPPT in PV system," *IEEE Trans. Ind. Informat.*, vol. 12, no. 1, pp. 187–200, Feb. 2016.
[32] S. Mohanty, B. Subudhi, and P. K. Ray, "A new MPPT design using grey wolf optimization technique for photovoltaic system under partial shading conditions," *IEEE Trans. Sustain. Energy*, vol. 7, no. 1, pp. 181–188, Jan. 2016.
[33] M. Seyedmahmoudian *et al.*, "Simulation and hardware implementation of new maximum power point tracking technique for partially shaded PV system using hybrid DEPSO method," *IEEE Trans. Sustain. Energy*, vol. 6, no. 3, pp. 850–862, Jun. 2015.
[34] X.-S. Yang and M. Karamanoglu, "Multi-objective flower algorithm for optimization," *Procedia Comput. Sci.*, vol. 18, pp. 861–868, Apr. 2, 2014.
[35] D. S. Niranjan, D. S. Bhaskar, M. J. Shekar, B. T. Sudhakar, and N. Rajasekar, "Solar PV array reconfiguration under partial shading conditions for maximum power extraction using genetic algorithm," *Renewable Sustain. Energy Rev.*, vol. 43, pp. 102–110, Mar. 2015.
[36] B. Indu Rani, G. Saravana Ilango, and C. Nagamani, "Enhanced power generation from PV array under partial shading conditions by shade dispersion using Su Do Ku configuration," *IEEE Trans. Sustain. Energy*, vol. 4, no. 3, pp. 594–601, Jul. 2013.

**J. Prasanth Ram** received the B.E. degree in electrical and electronics engineering from Bannari Amman Institute of Technology, Sathyamangalam, India, and M.E. degree in power electronics and drives from Kumaraguru College of Technology, Coimbatore, India, in 2012 and 2014, respectively. He is currently working toward the Ph.D. degree in solar PV systems at VIT University, Vellore, India.

His research interests include optimization techniques, power electronics, and applications of power electronics in renewable energy systems.

**N. Rajasekar** (M'13) was born in Erode, India, in 1979. He received the B.E. degree in electrical and electronics engineering from the University of Madras, Chennai, India and the M.E. degree in power electronics and drives from SASTRA University, Thanjavur, India, in 2000 and 2002, respectively, and the Ph.D. degree in electrical engineering from the National Institute of Technology, Trichy, India, in 2007.

From 2005 to 2010, he was working in the Institute of Road and Transport Technology, Erode. He is currently a Professor in the Department of Energy and Power Electronics, School of Electrical Engineering, VIT University, Vellore, India. His research interests include solar PV system, power electronics, application of power electronics in renewable energy sources, and dc–dc converters.

Dr. Rajasekar received "SOPHIA LECTURING—RESEARCH GRANT," from Sophia University, Japan.